

Feasibility of TEMPO-functionalized Imidazolium, Ammonium and Pyridinium Salts as Redox-Active Carriers in Ethaline Deep Eutectic Solvent for Energy Storage

Brian Chen,^{1,†} Sarah Mitchell,^{2,†} Nicholas Sinclair^{1,†}, Jesse Wainright^{1,*} Emily Pentzer,^{2,*} Burcu Gurkan^{1,*}

¹Department of Chemical Engineering Biomolecular Engineering, Case Western Reserve University, 10900 Euclid Avenue, Cleveland, Ohio 44106, United States

²Department of Chemistry, Department of Materials Science and Engineering, Texas A&M University, College Station, Texas 77840, United States

† These authors equally contributed

*Corresponding author: jsw7@case.edu, emilypentzer@tamu.edu; beg23@case.edu

Electronic Supplementary Information

Table of Contents:	Page
Materials	2
Instrumentation	3
Methods	3-11
Figure S1 (Calibration Curves for TEMPO derivatives)	12
Table S1 (Studied solutions)	13
Table S2 (Density Fitting Parameters)	14
Table S3 (Viscosity Fitting Parameters)	15
Table S4 (Ionic conductivity Fitting Parameters)	16
Figure S2 (CV of TEMPO in Acetonitrile)	17
Table S5 (Diffusion Coefficients)	17
Figure S3 (Electrochemical Windows of TEMPO derivatives)	18
Figure S4 (Current Density vs. Square Root of Scan Rate)	19
Figure S5 (T-Cell Representation)	19
Figure S6 (Example Nyquist Plot)	20
Scheme S1 (Deactivation of TEMPO ⁺)	20
Figure S7 (Chemical Characterization of Compound 1)	21
Figure S8 (Chemical Characterization of Compound 2)	22
Figure S9 (Chemical Characterization of Compound 3)	23
References	24

Materials

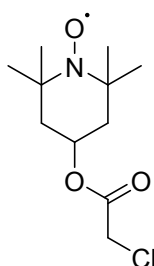
4-hydroxy-TEMPO (Sigma Aldrich, 97%), chloroacetic acid (Sigma Aldrich, 99%), 4-dimethylaminopyridine (Sigma Aldrich, 98%), and 1-methylimidazole (Sigma Aldrich, 99%), N,N'-dicyclohexylcarbodiimide (ACROS organics, 99%), ferric chloride hydrate (97%), trimethylamine (Fisher, 1M solution), and pyridine (fisher) were all used without further purification. All solvents for chemical synthesis were purchased from Fisher, unless otherwise stated. DCM and THF were obtained by passing commercial grade solvent through a column of activated neutral alumina in a Dow-Grubbs solvent system from Pure Process Technology (Nashua, NH). Choline Chloride, ChCl , ((2-hydroxyethyl)trimethyl)trimethylammonium chloride) (Acros Organics, 99%) was dried in a vacuum oven for over 12 hours at 150°C before use. Ethylene glycol, EG, (Acros Organics, anhydrous, 99%) was used without further purification. 4-hydroxy-TEMPO, 4HT, (Alfa Aesar, 98%) was recrystallized using hexane at 50°C. TEMPO (Sigma Aldrich, 99%), however, was not recrystallized because it can sublime in a vacuum. Each synthesized TEMPO derivate was dried in a vacuum oven for over 12 hours at 80°C. Acetonitrile (Alfa Aesar, 99.8%, 75-05-8) was used without further processing. Heat shrink tubing (NTE Electronics, 47-20306-CL) was used in preparation of reference and counter electrodes. An argon-filled glovebox (VTI Super, > 1 ppm water and oxygen) was used to handle all DES samples and DES constituents. Pt wire (Alfa Aesar, 0.3 mm dia., 99.9%) for cyclic voltammetry.

Instrumentation

Elemental analysis was used to confirm the purity of the synthesized TEMPO derivatives, as shown in the supporting information. ^1H Nuclear magnetic resonance (NMR), ^{13}C NMR, fourier transform infrared spectroscopy (FTIR), and electron spray ionization (ESI) was performed for compound **1**, **2**, and **3**. Due to compounds **1**, **2**, and **3** being paramagnetic, phenylhydrazine was added to each NMR sample to obtain the spectra. All ^1H , ^{13}C , ^{29}Si NMR were collected on Bruker Ascend III HD 500MHz NMR instrument equipped with prodigy probe and shifts are reported relative to residual solvent peak, as noted. All NMR spectra were collected using CDCl_3 as the solvent unless otherwise noted. FTIR spectra were acquired using an Aglient Cary 630 FT-IR in ATR mode. ESI spectra were obtained on THERMO Finnigan LCQ DECA ion trap mass spectrometer equipped with an external AP ESI ion source. All UV-Vis spectra was obtained on a Cary 5000 UV-Vis-NIR.

Methods

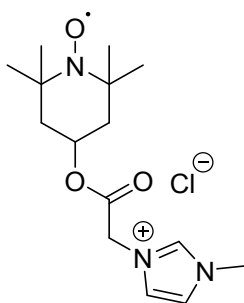
Preparation of TEMPO-chloroacetate intermediate^{1,2}



An oven-dried round bottom flask (RBF) was purged with vacuum and N_2 . 4-hydroxy TEMPO (2.18g, 0.025mol) and chloroacetic acid (1.20g, 0.025mol) were added to the flask, followed by dichloromethane (DCM) (30mL). The flask was cooled to 0°C with an ice water bath under N_2 . 4-Dimethylaminopyrdine (DMAP, 0.39g, 0.006mol) and N,N'-dicyclohexylcarbodiimide (DCC, 2.62g, 0.025mol) were dissolved with DCM (15mL) and the solution added dropwise. Once added, the reaction was warmed to room temperature and stirred for 5 hrs at 400rpm. Upon completion,

the reaction was cooled to 0°C with an ice water bath, the white precipitate was filtered with a Buchner funnel. The filtrate was washed with 1M HCl (25mL), saturated NaHCO₃ (25mL), and saturated NaCl (25mL) (chilling and filtering organic layer between each wash). The organic layer was dried over magnesium sulfate and solvent removed under reduced pressure using the rotary evaporator. The product was purified through column chromatography, eluted with a 9:1 hexane: ethyl acetate. Solvent was removed under reduced pressure and the product dried under vacuum. Product was an orange solid, with a 77% yield (2.5g).

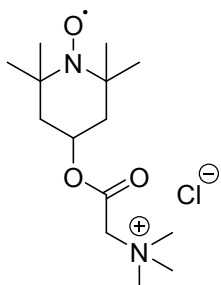
Preparation of Compound 1



In an oven-dried RBF, TEMPO-chloroacetate intermediate (1.0 g, 0.004 mol) was dissolved in acetonitrile (30mL). 1-methylimidazole was added slowly. The reaction was heated to 60°C and stirred at 400 rpm for 48hrs.

Reaction was monitored with thin layer chromatography (TLC). Upon completion, the reaction was cooled with an ice water bath and diethyl ether (30 mL) was added. The precipitate was filtered and washed with acetone (40mL) and diethyl ether (40mL) successively. The product obtained was as red powder and dried under vacuum in 83 % yield (1.1g).

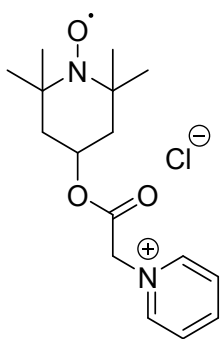
Preparation of Compound 2



In an oven-dried RBF, TEMPO-chloroacetate intermediate (0.79g, 0.0032 mol) was dissolved in dry tetrahydrofuran (20 mL). A solution of 1M trimethylamine in THF (2.23mL, 0.046mol) was added slowly. The reaction was stirred at room temperature at 400 rpm for 24hrs under N₂(g).

Reaction was monitored with TLC. Once complete the reaction was cooled with an ice water bath and diethyl ether (30 mL) was added. The precipitate was filtered and washed with acetone (50 mL) successively. The product obtained was a red powder in 57% yield (0.56g) and dried under vacuum.

Preparation of Compound 3



In an oven-dried RBF TEMPO-chloroacetate intermediate (3.0g, 0.012 mol) was dissolved in acetonitrile (70 mL). Pyridine (1.2mL, 0.015 mol) was added slowly. The reaction was heated to 60°C and stirred at 400 rpm for 72 hrs. Reaction was monitored with TLC. Once complete the reaction was cooled with an ice water bath and ethyl acetate (100mL) was added. The precipitate was filtered and washed with acetone (50mL) and diethyl ether (50mL) successively. The product obtained was a red powder in 49 % yield (1.95g) and dried under vacuum.

Preparation of ethaline and redox-active DESs

Ethaline was prepared by mixing 1:2 molar ratio of choline chloride (ChCl) to ethylene glycol (EG) stirring at 80°C and 300 rpm for 30 minutes in a 20 mL glass vial. In a typical ethaline preparation, approximately 10.12 g of ChCl was mixed with 9.03 g of EG to make a 1:2 molar ratio of ChCl to EG. The hot plate was turned off and the solution was cooled slowly to room temperature. In a typical redox-active DES preparation, 0.16 g of TEMPO was mixed with 7.79 g of ethaline to make a 0.15 M concentration of TEMPO in ethaline. Water contents of the ethaline stock solution and the redox-active DES solutions prepared from TEMPO, 4HT and derivatives **1**, **2**, **3** at

concentrations ranging from 0.25-1.2 M were measured by a Karl Fischer titrator (Metrohm Coulometric KF 899 D) as shown in **Table S1**.

Solubility measurements

Solubility limits of TEMPO and TEMPO derivatives in ethaline were determined by calibration curves obtained from UV-Vis (**Figure S1**). Five solutions of pre-determined concentration were made for each compound in DMSO. The UV-vis spectra were taken from 200-800nm. The calibration curves were plotted at a specific absorption wavelength for each compound. To make the concentrated samples, each TEMPO derivative was added to ethaline (0.5mL) and heated on a hot plate. This process was repeated till solid remained present in solution. The saturated samples were cooled to room temperature and stood for at least one hour. A solution was made with DMSO and UV-vis obtained from 200-800nm. The solubility limit was obtained as in **Table S1**.

Density

Densities were measured with an oscillating U-tube density meter (Anton Paar DMA 4500) from 25 – 55°C with an uncertainty of $\pm 0.0005 \text{ g cm}^{-3}$. A linear line fit was performed to determine the temperature dependence of density according to (1):

$$\rho = A + BT \tag{1}$$

where $\rho \text{ (g cm}^{-3}\text{)}$ is the density at temperature $T \text{ (K)}$ and A and B are fitting parameters.

Viscosity

Viscosities were measured by a microchannel viscometer (MicroVISC, Rheosense) at a temperature range of 25 – 55°C. Approximately 10-45 μL of solution was injected into the microchannel with a flow rate between 10-450 $\mu\text{L min}^{-1}$ for all measurements. At each temperature, the viscosity was measured in triplicate and the variability was observed to be 5 %. The temperature dependence of viscosity was obtained by the Vogel-Fulcher-Tamann (VFT) model shown in (2):

$$\eta = \eta_o \exp\left(\frac{B_\eta}{T - T_o}\right) \quad (2)$$

where η (cP) is the viscosity at temperature T (K), η_o (cP) is the pre-exponential factor, B_η (K) is activation temperature and T_o (K) is the ideal glass transition temperature.

Ionic Conductivity

The ionic conductivities were measured by electrochemical impedance spectroscopy (EIS) using a potentiostat equipped with frequency response analyzer (BioLogic SP 240). A two-electrode cell (Biologic MCM-CC) with parallel, non-platinized Pt electrodes was used as for the conductivity measurements. A 0.1 M $\text{KCl}_{(\text{aq})}$ solution was used to determine the conductivity cell constant (1.38 cm^{-1}). About 600 μL of sample was loaded into the conductivity cell inside an argon-filled glovebox. The voltage amplitude was set at 10 mV and the applied frequency range was 100 kHz to 100 Hz from 25 – 55°C. For every sample, EIS was repeated three times. The bulk resistance of each sample was determined from the real intercept of Nyquist plot where the imaginary impedance is plotted with respect to the real part of the impedance (See **Figure S6**). The x-

intercept of the fitted line was taken as R_b , the resistance of the bulk solution. The ionic conductivity was then calculated using (3):

$$\sigma = \frac{d}{R_B A} = \frac{\text{Cell Constant}}{R_B} \quad (3)$$

where d (cm) is the distance between the two parallel Pt electrodes, R_b (ohm) is the bulk resistance of the solution and A (cm²) is the area of the Pt electrode. The ratio d/A constitutes the cell constant. The VFT model was used to express temperature dependence of conductivity shown in (4):

$$\sigma = \sigma_o \exp\left(\frac{B_\sigma}{T - T_o}\right) \quad (4)$$

where σ is the conductivity (mS/cm) for temperature T (K), σ_o (mS/cm) is the pre-exponential, B_σ (K) is the activation temperature and T_o (K) is the ideal glass transition temperature obtained from the viscosity VFT fit.

Electrochemical Characterization: Electrochemical Window and Diffusivity

Unless noted otherwise, cyclic voltammetry (CV) was performed in a 3-electrode cell inside an Argon purged glovebox (VTI Super, 1 > ppm water and oxygen) to determine the electrochemical windows (EW) and study the redox potentials and reversibility of DESs with TEMPO functionality. A glassy carbon disc electrode (BASi MF-2012, 3 mm dia, surface area = 0.0707 cm²) was used as the working electrode. Pt wire was used as the counter electrode, and Ag/AgCl wire was the reference electrode. The Ag/AgCl wire reference electrode was prepared using chronoamperometry as described in Shen *et al.*³, where the chloride containing solution for AgCl

deposition was ethaline. The step potential for AgCl deposition was +1.5 V versus a graphite rod.

With the exception of the microelectrode experiments, the electrodes were arranged in a T-cell configuration for CVs (**Figure S5**). The fabricated Ag/AgCl reference electrode was first wrapped with Teflon tape and then isolated from the coiled Pt counter electrode around it with heat-shrink tubing. The Pt-wire counter electrode was wound around the first layer of heat-shrink tubing along the length of the Ag/AgCl wire, and then coiled eight times near the tip of the exposed Ag/AgCl wire. The counter and reference electrodes were then placed over the working electrode with approximately 0.5 cm distance between the reference and the working electrode. About 200 μL of solution was injected into the liquid reservoir over the working electrode (created by heat-shrink tube) for each CV measurement. Before each measurement, the glassy carbon disk electrode was polished with 0.05 μm alumina suspension (BASi, CF-1050) and ultrasonicated with deionized (DI) water. All CV measurements are iR-compensated (85%). For the iR-compensation, EIS was performed with 100 kHz single-frequency and a voltage amplitude of 20 mV. EW was determined using a scan rate of 10 mV s^{-1} from -2.5 V to +1.5 V vs. Ag/AgCl. 50 cycles were performed to confirm redox reversibility within the potential region of interest that is identified from the initial EW measurements. The CV measurements for studying the redox reactions were started from open circuit potential and then scanned to the negative direction to -1.5 V and then scanned to the positive direction to +1.1 V vs. Ag/AgCl. CV was performed for 50 cycles between -1.5 V to +1.1 V vs. Ag/AgCl.

Diffusion coefficients of redox active solutes were measured using CV at a restricted potential range from +0.5 V to +1.1 V. Like the EW measurements, voltammetry measurements for measuring diffusion coefficient were started from open circuit potential and scanned to the positive direction that includes the redox potentials of TEMPO and derivatives in ethaline. Scan rates of 5, 10, 20, 50, 100, and 200 mV s⁻¹ were used for application of the Randles-Sevcik (5):

$$i_p = 0.4463nFAC\left(\frac{nFvD}{RT}\right)^{\frac{1}{2}}$$

(5)

where A (cm²) is the electro-active surface area of the working electrode (A = 0.0707 cm²), C (mol cm⁻³) is the bulk concentration of the redox-active small molecule salt, v (V s⁻¹) is the scan rate, D (cm² s⁻¹) is the diffusion coefficient of the redox active solute and i_p (mA cm⁻²) is the peak current density. **Figure S4** illustrates the application of the Randles-Sevcik equation in estimating the diffusion coefficients reported.

Flow Cell Experiments

Flow cell testing was performed using an in house 2.5 cm² flow cell design. The cell uses a flow through electrode configuration. Graphite current collectors were machined in-house from impervious graphite (Graphite Store). Morgan Advanced Materials WDF 3 mm thick felt compressed to 2.5 mm was used as the flow through electrode. The felts were heat treated at 400 °C for 4 hours prior to use in the flow cell to improve their wettability. Polyvinyl-alcohol hydrogel coated Daramic 175 (200 μm wetted thickness) was used as a porous separator.⁴ This separator was developed in house. The Daramic was soaked in 2-propanol for 10 minutes to

remove residual oil remaining after manufacture and then dried in air prior to use. Charging of the electrolyte was performed with a constant current of 20 mA/cm² at 22°C to ensure that at 0% SOC the cell overpotential was less than 200 mV. A constant electrolyte flow rate of 40 mL/min was used. A 20 ml sample takes approximately 1.3 hours to charge to 50% SOC under these conditions with a final overpotential of approximately 400 mV. All 'dry' flow cell experiments were performed in a nitrogen purged, dry glove box with an approximate dew point of -75 °C.

The voltammetry of the positive and negative electrolytes following a flow cell experiments was performed on with 100 µm diameter platinum microdisk purchased from BASi. A platinum mesh counter electrode was used. A chloridized silver wire placed directly into the electrolyte was used as reference for all three electrode experiments. Aqueous microelectrode voltammetry was performed using a similar working and counter electrode but with a commercial Ag/AgCl reference electrode purchased from BASi. Microelectrode CVs and flow cell experiments were performed with a Solartron 1280B Potentiostat.

For the microelectrode CVs, the following equation holds at sufficiently slow scan rates:

$$i_{ss} = 4nFDcR \quad (6)$$

where i_{ss} is the steady state current determined from the voltammetry, n is the number of electrons transferred, F is Faraday's constant, D is the diffusion coefficient of the active species, C is the bulk concentration of the active species and r is the radius of the micro-disk. For a viscous electrolyte such as used here, the diffusion coefficient of the reacting species is small enough

that true steady-state behavior is only observed at very slow scan rates, on the order of 0.5 mV/s.

However, at 5 mV/s as shown in **Figure 6**, the current observed on the reverse scans are steady and consistent with the micro-disk equation.

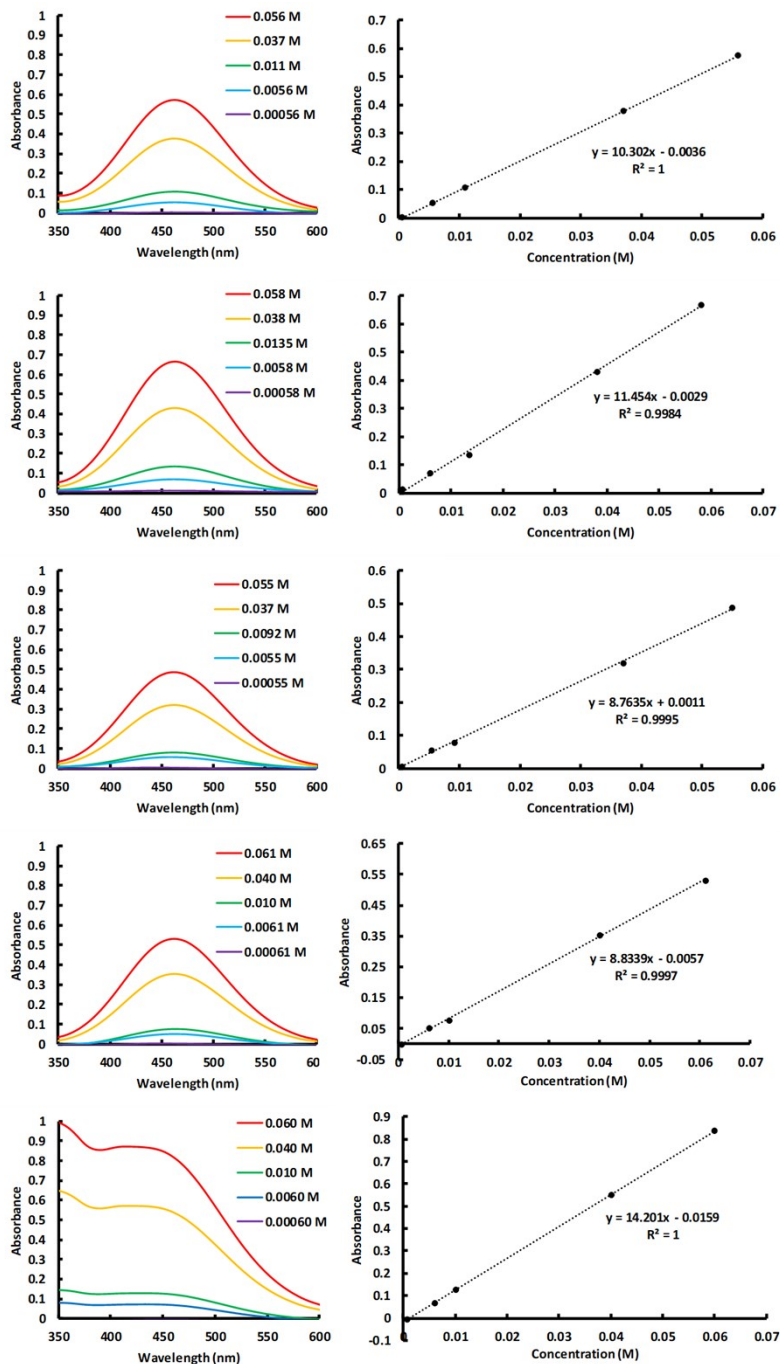


Figure S1. UV-Vis spectra of saturated solutions of TEMPO and its derivatives in in DMSO, calibration curves, and UV-Vis spectra of saturated solutions of TEMPO and its derivatives in ethaline for (a) TEMPO, (b) 4HT, (c) **1**, (d) **2**, and (e) **3**.

Table S1. Structure, molecular weight (MW), solubility, melting point (T_m), and the decomposition temperature (T_{0.05}loss: temperature corresponding to 5 w% mass loss during the Thermal Gravimetric Analysis) of the redox active compounds studied in ethaline. The prepared solution concentrations of the compounds in ethaline for physical property and electrochemical characterization are provided with their respective water content, measured by KF titrator.

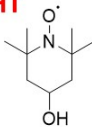
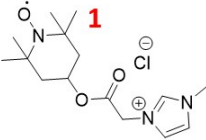
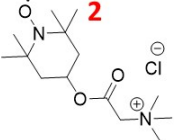
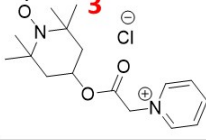
Compound	MW (g/mol)	Solubility in ethaline (mol/L)	T _m (°C)	T _{0.05} loss (°C)	Solutions studied (mol/L)	Water content (ppm)
TEMPO 	156	0.17	36-38	--	0.05	136.6
					0.10	120.7
					0.15	113.2
4HT 	172	1.93	69-71	155.5	0.5	178.6
					0.8	148.1
					1.2	74.0
1 	330	0.94	209-212	244.5	0.25	210.8
					0.5	141.6
					0.8	117.5
2 	307	1.35	165-174	199.1	0.5	274.2
					0.8	260.7
					1.2	387.2
3 	327	0.85	200-204	224.8	0.25	77.6
					0.5	105.2
					0.8	114.8

Table S2. Linear fit parameters for the temperature dependence of the measured densities ($R^2 > 0.999$ for all solutions).

$\rho = A + BT$			
Compound	Concentration (M)	A (g cm^{-3})	B x 10^{-4} ($\text{g cm}^{-3} \text{ }^\circ\text{C}^{-1}$)
TEMPO	0.05	1.13029	-5.675
	0.10	1.12917	-5.682
	0.15	1.12790	-5.688
4-hydroxy-TEMPO	0.5	1.12594	-5.755
	0.8	1.12273	-5.808
	1.2	1.11793	-5.887
1	0.25	1.13520	-5.762
	0.50	1.13695	-5.684
	0.80	1.14371	-5.767
2	0.50	1.13284	-5.698
	0.80	1.13213	-5.658
	1.2	1.13442	-5.677
3	0.25	1.13510	-5.696
	0.50	1.13736	-5.643
	0.80	1.14321	-5.692

Table S3. VFT fit parameters for temperature dependence of the measured viscosities ($R^2 > 0.998$ for all solutions).

$$\eta = \eta_o \exp\left(\frac{B_\eta}{(T - T_o)}\right)$$

Compound	Concentration (M)	η_o (cP)	B_η (K)	T_o (K)
TEMPO	0.05	0.58	-455.88	195.80
	0.10	0.56	-474.46	192.69
	0.15	0.08	-1075.37	134.81
4HT	0.5	0.25	-688.30	171.84
	0.8	0.12	-921.71	151.55
	1.2	0.58	-485.13	197.77
1	0.25	0.16	--811.43	163.13
	0.50	0.37	-634.29	181.30
	0.80	1.67	-366.28	212.33
2	0.50	0.66	-462.21	199.73
	0.80	0.14	-883.75	162.50
	1.2	0.68	-512.27	204.84
3	0.25	0.52	-487.13	196.46
	0.50	0.04	-1409.80	114.18
	0.80	0.12	-970.29	158.76

Table S4. VFT fit parameters for temperature dependence of the measured conductivities ($R^2 > 0.990$ for all solutions). T_0 is the same as in **Table S3**.

$$\sigma = \sigma_o \exp\left(\frac{B_\sigma}{(T - T_o)}\right)$$

Compound	Concentration (M)	σ_o (mS cm ⁻¹)	B_σ (K)
TEMPO	0.05	340.88	393.55
	0.10	411.77	429.59
	0.15	1747.82	902.01
4HT	0.5	533.98	564.86
	0.8	1902.82	867.42
	1.2	311.36	425.97
1	0.25	1296.52	725.90
	0.50	611.88	568.28
	0.80	243.94	368.80
2	0.50	367.59	427.25
	0.80	1589.92	824.71
	1.2	331.21	461.07
3	0.25	400.13	430.63
	0.50	7163.30	1347.60
	0.80	4152.81	767.82

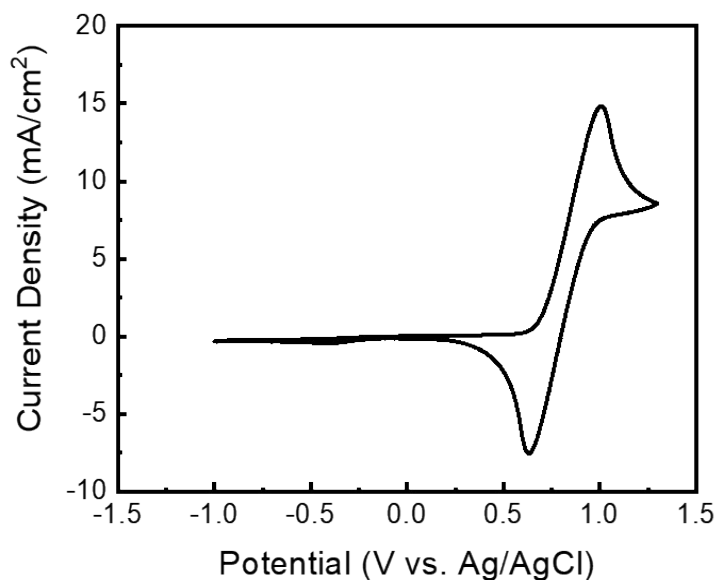


Figure S2. Voltammetry of 50 mM TEMPO in acetonitrile with 100 mM TEAP supporting electrolyte. Scan rate is 100 mV s⁻¹.

Table S5. Measured diffusion coefficients (D), Cathodic (E_{cathodic}) and anodic (E_{anodic}) limits, electrochemical windows (EW) and oxidation (E_{ox}) and reduction (E_{red}) potentials of TEMPO for E_1 . All potentials are vs. Ag/AgCl and with a cut-off current density of 0.5 mA cm⁻². D was calculated using Randles-Sevcik equation from the 1st CV cycle (**Figure S3**) of 0.5 M solutions.

	$D \times 10^{-8}$ (cm ² s ⁻¹)	E_{anodic} (V)	E_{cathodic} (V)	EW (V)	E_{ox} (V)	E_{red} (V)
4HT	4.37	+1.27	-1.96	3.23	+0.88	+0.71
1	1.48	+1.29	-1.99	3.28	+0.91	+0.74
2	2.43	+1.22	-1.71	2.93	+0.88	+0.73
3	1.44	+1.24	-1.27	2.51	+0.91	+0.75

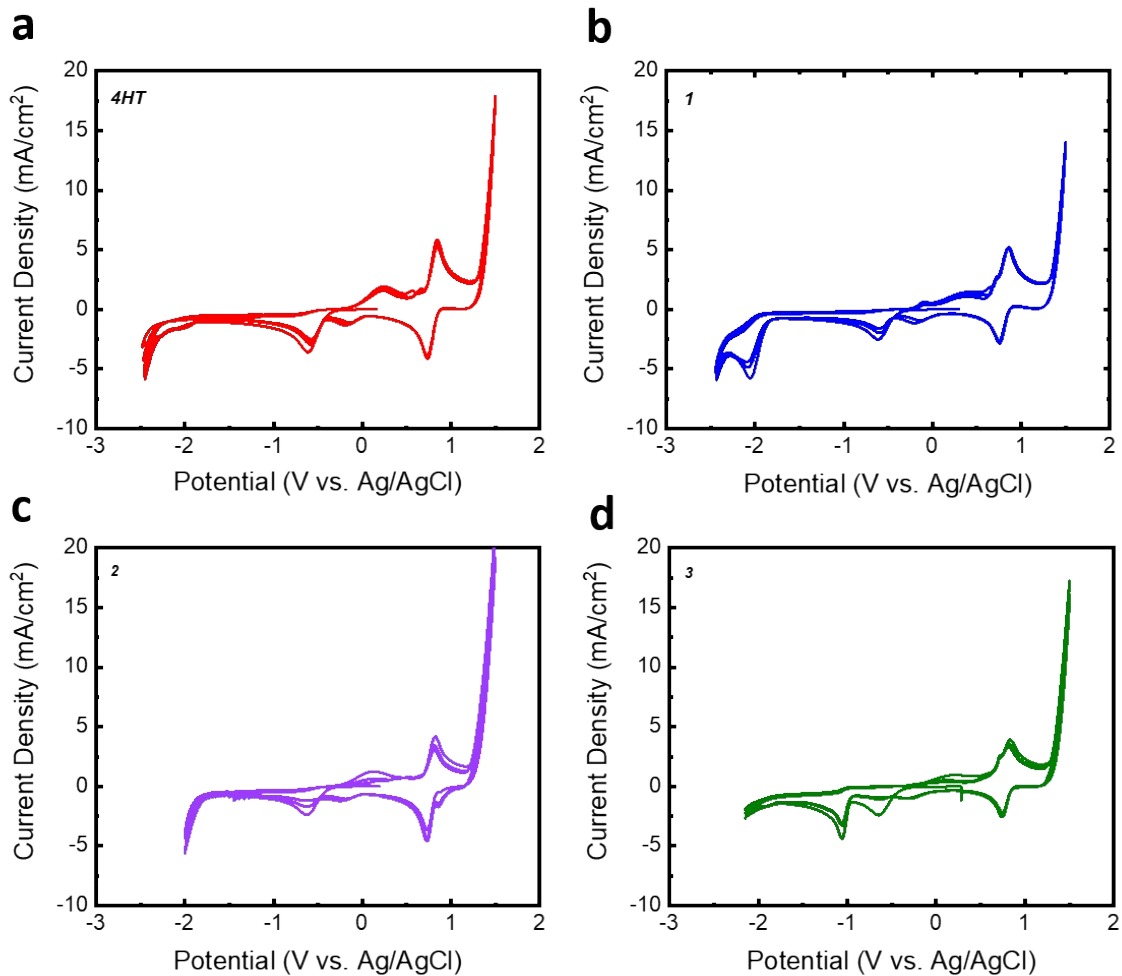


Figure S3. Electrochemical windows of 0.5 M concentration (a) 4HT, (b) 1, (c) 2, and (d) 3 dissolved in ethaline. Three full cycles are shown at a scan rate of 10 mV s⁻¹.

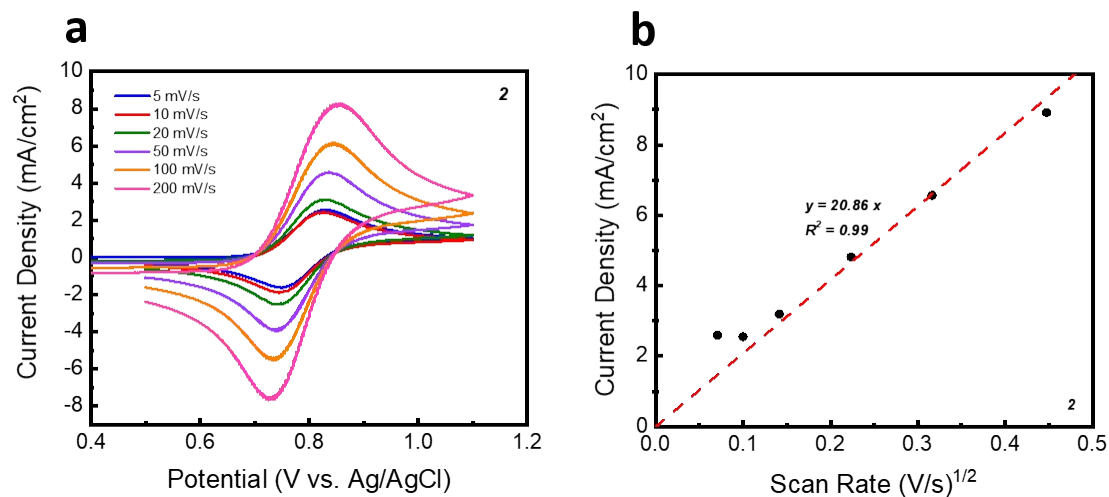


Figure S4. (a) CV of compound 2 (0. 5M in ethaline) at various scan rates; (b) Current density vs. square root of scan rate. The dashed line demonstrates the linear fit for the estimation of the diffusion coefficients according to Randles-Sevcik equation (5).

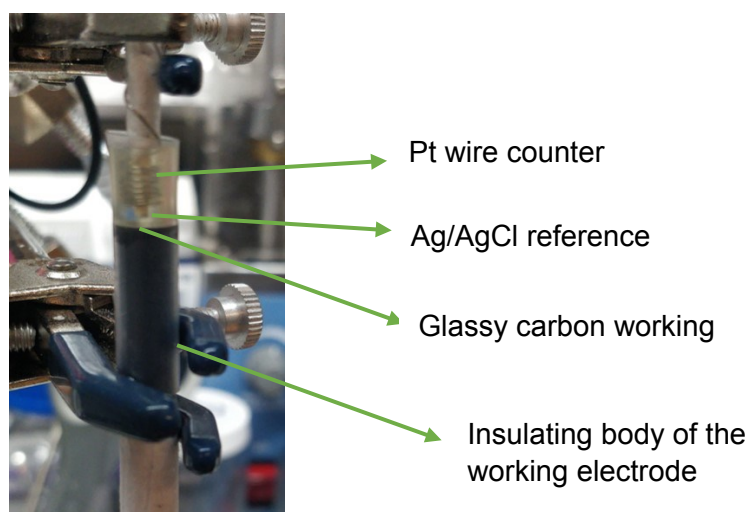


Figure S5. T-cell used for cyclic voltammetry. Shown is a Pt-wire coil counter electrode around the Ag/AgCl reference (separated by an insulator) on top of the disc glassy carbon working electrode. The liquid is housed in the reservoir on top of the working electrode created by heat shrink tube around the insulator body of the working electrode.

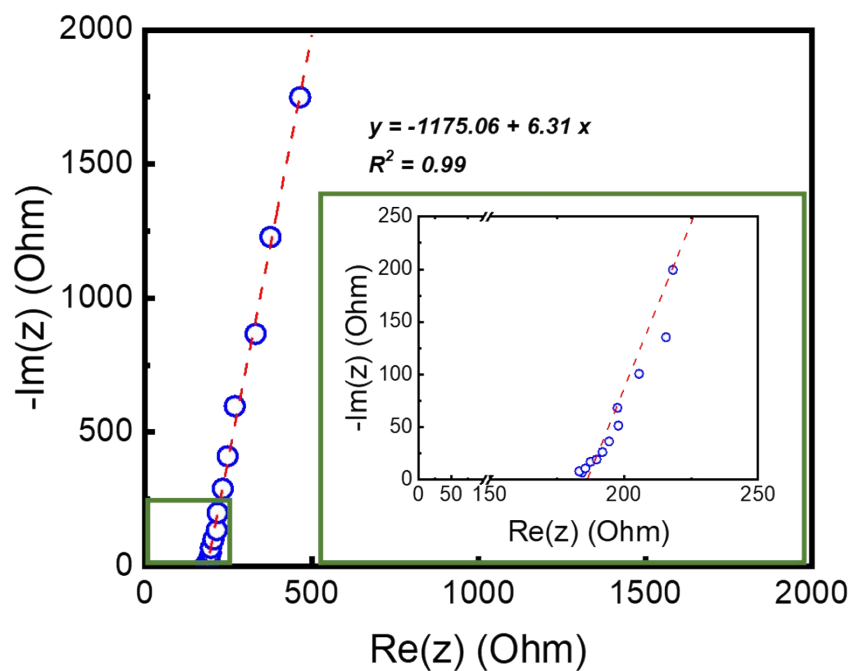
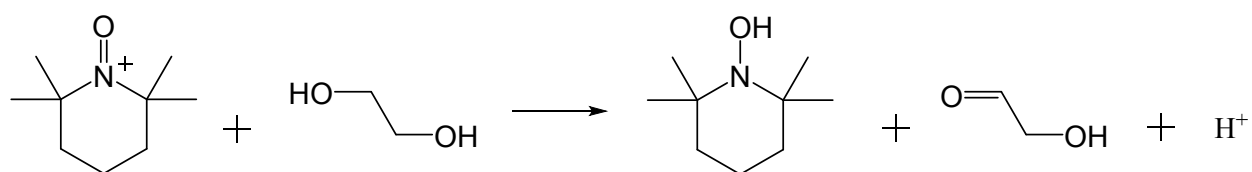


Figure S6. Nyquist plot for ethaline from electrochemical impedance spectroscopy. Voltage Frequency range is 100 kHz - 100 Hz. Inset displays the x-intercept of the linear fit representing the bulk resistance for conductivity calculations.

Scheme S1. Possible deactivation (electrochemical) reaction of TEMPO⁺ in ethylene glycol



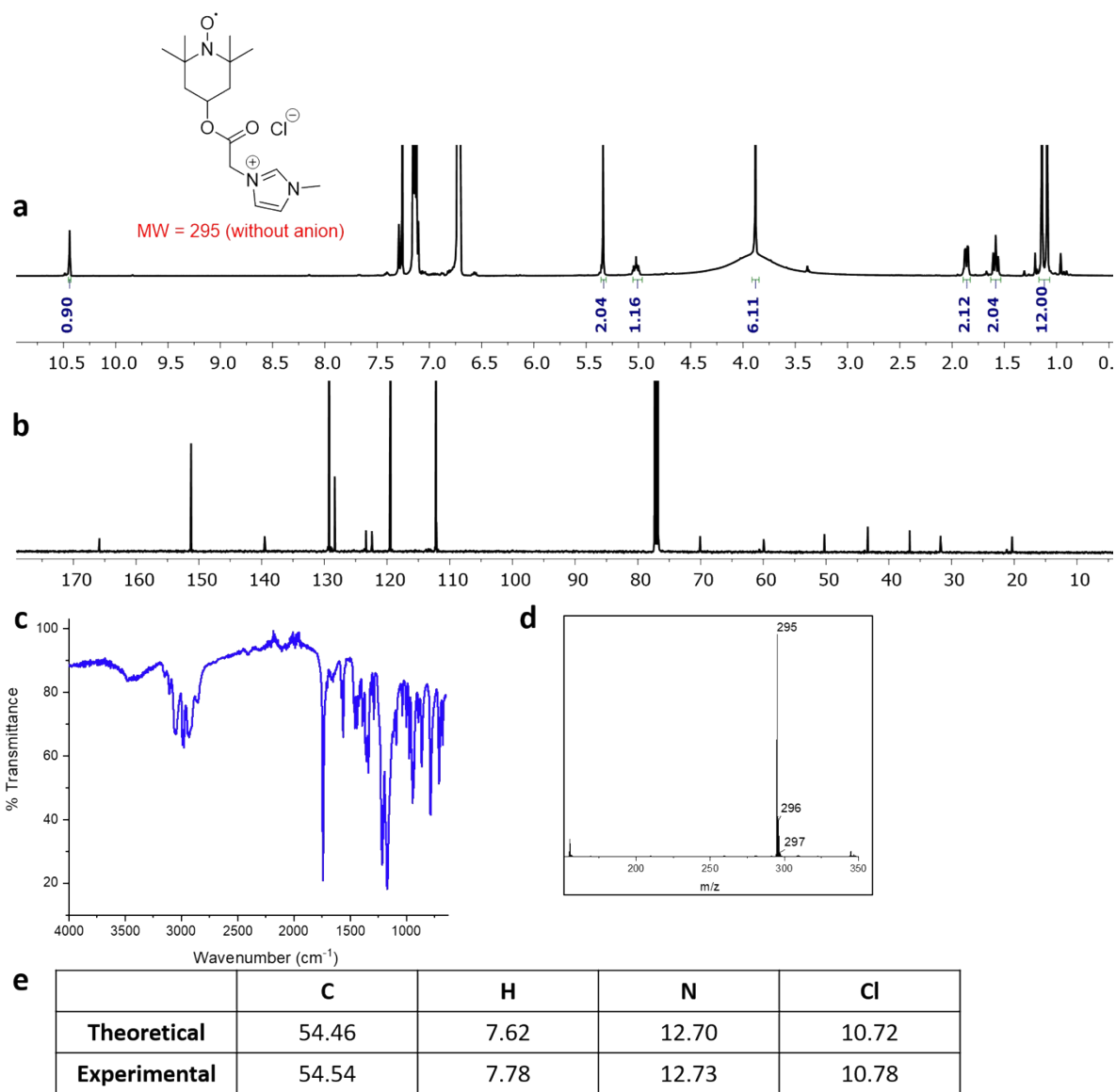


Figure S7. Chemical characterization of compound **1**. (a) ^1H NMR, (b) ^{13}C NMR, (c) FTIR, (d) ESI, (e) elemental analysis.

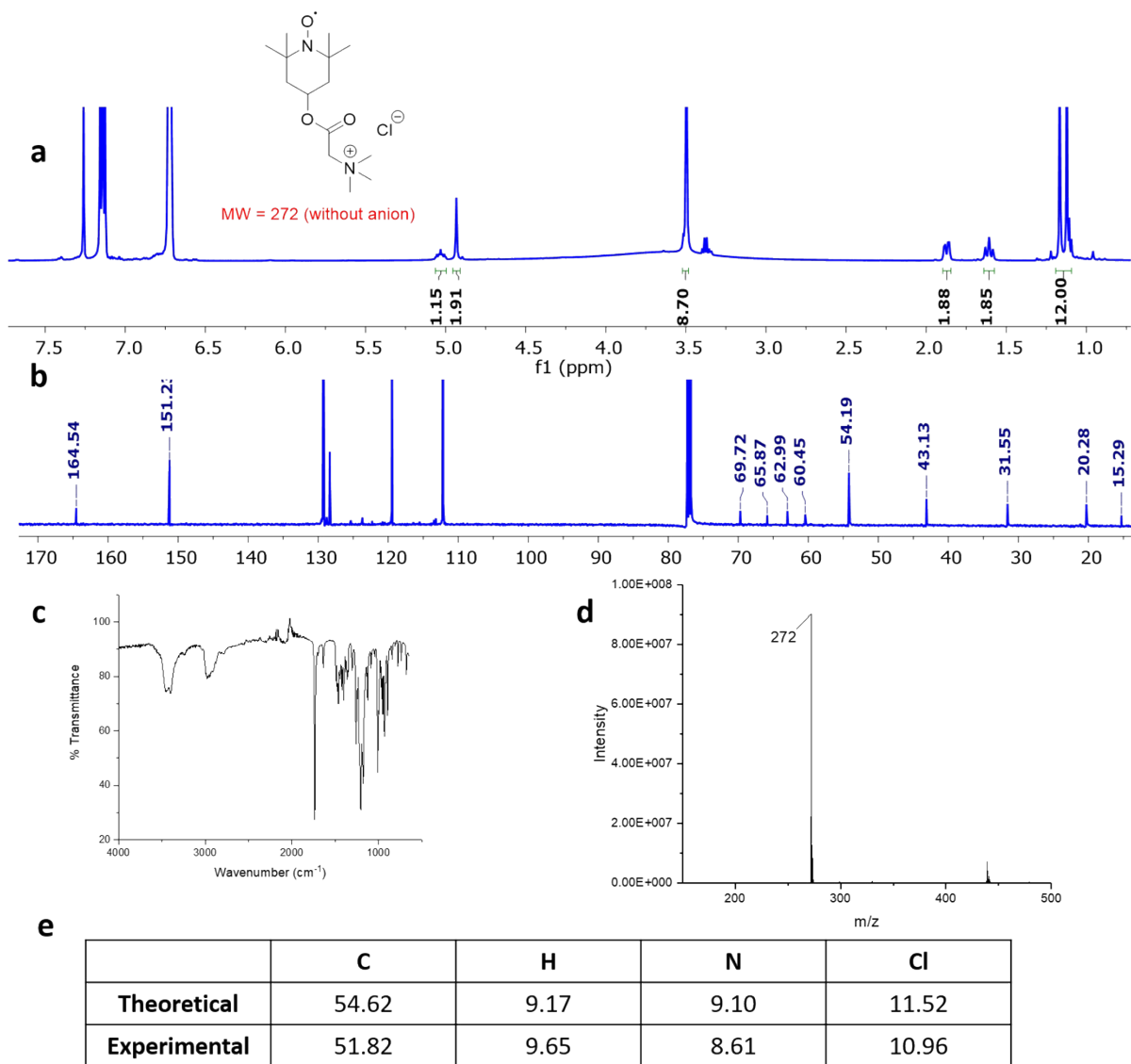


Figure S8. Chemical characterization of compound **2**. (a) ^1H NMR, (b) ^{13}C NMR, (c) FTIR, (d) ESI, (e) elemental analysis.

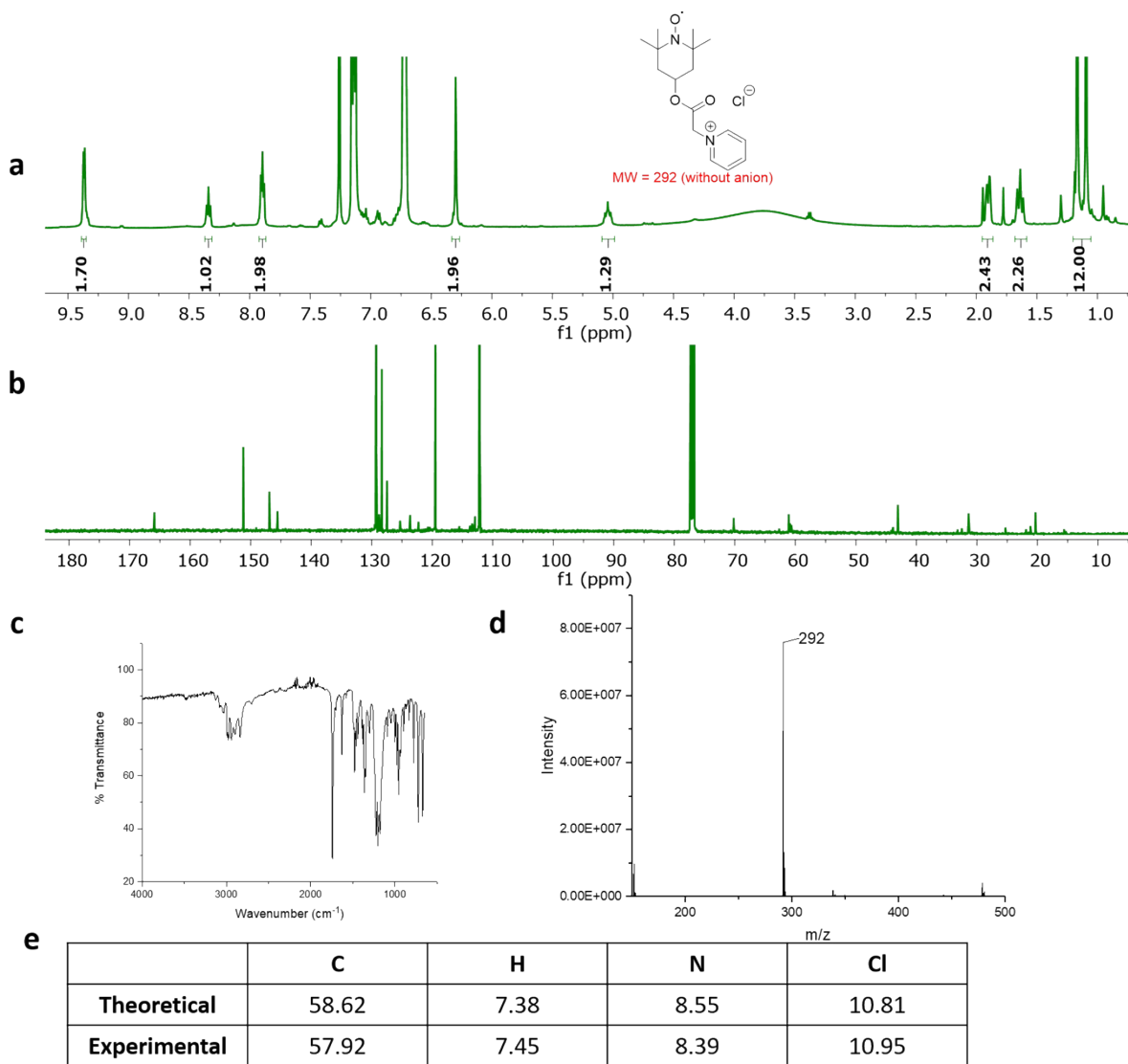


Figure S9. Chemical characterization of compound **3**. (a) ^1H NMR, (b) ^{13}C NMR, (c) FTIR, (d) ESI, (e) elemental analysis.

References

- (1) Wu, X.-E.; Ma, L.; Ding, M.; Gao, L. TEMPO-Derived Task-Specific Ionic Liquids for Oxidation of Alcohols. *Synlett* **2005**, *4*, 607–610.
- (2) Miao, C.; Wang, J.; Yu, B.; Cheng, W.; Sun, J.; Chanfreau, S.; He, L.-N.; Zhang, S.-J. Synthesis of Bimagnetic Ionic Liquid and Application for Selective Aerobic Oxidation of Aromatic Alcohols under Mild Conditions. *Chem. Commun.* **2011**, *47*, 2697–2699.
- (3) Shen, D.; Steinberg, K.; Akolkar, R. Avoiding Pitfalls in the Determination of Reliable Electrochemical Kinetics Parameters for the $\text{Cu}^{2+} \rightarrow \text{Cu}^{1+}$ Reduction Reaction in Deep Eutectic Solvents. *J. Electrochem. Soc.* **2018**, *165* (14), E808–E815.
- (4) Selverston, S., Nagelli, E., Wainright, J. S., Savinell, R. F, All-Iron Hybrid Flow Batteries with In-Tank Rebalancing, *Journal of The Electrochemical Society*, **2019**, *166* (10) 1725-1731